Weighted-average model curve preprocessing strategy for quantification of DSC perfusion imaging metrics from image-guided tissue samples in patients with brain tumors

Janine M Lupo[1], Qiuting Wen[1], Joanna J Phillips[2,3], Susan M Chang[2], and Sarah J Nelson[1]

[1]*Radiology and Biomedical Imaging, University of California, San Francisco, CA, United States,* [2]*Neurological Surgery, University of California, San Francisco, CA, United States,* [3]*Pathology, University of California, San Francisco, CA, United States*

Introduction

Tissue heterogeneity of glioblastoma multiforme (GBM), a highly malignant and vascularized human brain tumor, has historically been a challenge for selecting biopsy tissue samples for tumor grading that accurately represent the tumor biology. The growing number of institutions performing image-guided collection of tissue samples along with the emergent widespread clinical availability of physiological imaging techniques such as diffusion- and perfusion-weighted MR imaging, have made apparent the need for standardization of both acquisition and post-processing protocols to accurately quantify metrics that reflect the underlying the tissue histopathology. Dynamic susceptibility-contrast (DSC) MRI if often the tool of choice to noninvasively assess tumor vasculature, and has been shown to result in metrics that are associated with increased microvascular density, proliferation, and abnormal morphology [1-3]. Despite the differences in acquisition (ie. administering a pre-dose of contrast agent, using a dual echo sequence, or applying a lower flip angle) and post-processing strategies (ie. gamma-variate fitting or baseline subtraction) to correct for the T1-effects of extravascular leakage on blood volume estimates [4-6], all of these approaches suffer from the same limitations of off-resonance effects and lower spatial resolution that are inherent to an echo planar imaging sequences. This results in small regions of interest, such as image-guided biopsied tissue samples, being highly sensitive to the resolution at which the analysis is performed. Neighboring regions of necrosis or susceptibility artifacts present within the tumor can exacerbate this variability, resulting in voxels with time courses of noise adversely affecting the overall sample quantification. In this study we propose a new method for pre-processing DSC data collected preoperatively for the analysis of image-guided tissue samples and compare the variability of resulting blood volume metrics with two approaches commonly used for quantification of perfusion metrics from image-guided tissue samples. The correspondence of parameter distribution with histopathological measures of vascular morphology was also evaluated for the different pre-processing strategies.

Methods

79 image-guided tissue samples from 40 patients newly-diagnosed with GBM were retrospectively analyzed in conjunction with preoperative DSC perfusion imaging. Preoperative 3T MR exams included T2* DSC gradient-echo echo-planar imaging (flip angle=35°, TE/TR=54–56/1250-1500ms, slice thickness=3-4 mm, 2x2mm reconstructed in-plane resolution, 0.1mmol/kg Gd-DTPA) as well as 3D-anatomic (pre- and post-contrast T1-weighted SPGR, T2-weighted FLAIR, FSE), diffusion-weighted, and spectroscopic imaging. The DSC data were nonrigidly aligned to the pre-contrast, T1-weighted images using B-spline warping by maximization of normalized mutual information to minimize distortion from the echo-planar imaging [7]. A 5-mm diameter spherical mask was generated at the resolution of the post-contrast T1 image (1x1x1.5mm), which was utilized during surgery to record the center coordinates of the extracted tissue sample using a BrainLab VectorVision Surgical Navigation System. Pre-processing of DSC data was performed in 3 different ways: 1) resampling the low resolution perfusion images to the high resolution post-contrast T1 image via tri-linear interpolation (TLI); 2) reformatting the high resolution tissue sample masks to the low resolution perfusion data using nearest-neighbor interpolation (NNI); and 3) through generation of a weighted-average model-curve (WAM). Parameter maps calculated from the TLI and NNI methods are then averaged within the tissue sample mask at the corresponding resolution, while the WAM method determines the percentage of the tissue sample mask within each perfusion voxel and automatically excludes unquantifiable voxels of noise[8] before taking a weighted average of the remaining dynamic curves based on the percentage overlap with the mask to create one curve per tissue sample to quantify. The resulting increase in SNR of the dynamic data in turn improves the accuracy or goodness of fit of model fitting for cerebral blood volume (CBV) calculation. Both nonlinear gamma-variate fitting with subsequent leakage correction[6] and non-parametric[8] post-processing methods were subsequently applied to the output of each pre-processing strategy to generate metrics of CBV, peak height (PH), and percent signal recovery (%REC) for each tissue sample. All PH and CBV values were normalized by respective values from normal-appearing brain tissue obtained via histogram analysis [8]. An overall microvascular morphology score was assigned to each tissue sample using Factor VIII immunohistochemical (IHC) staining based on the most abnormal morphologic-type of vasculature present: 'delicate' normal vessels; 'simple' microvascular hyperplasia; or 'complex' microvascular hyperplasia.

Results & Discussion

Variability in Parameter Estimation: Figure 1A shows decreased variability in both nPH (top panel) and %REC (bottom panel) values between nonlinear and nonparametric estimates when using the WAM pre-processing method. The R-squared values of the linear regression between PH and %rec parameters quantified by nonlinear fitting and nonparametric curve analysis were significantly elevated with the WAM method (.95-WAM vs .84-NNI and .51-TLI for PH; and (.94-WAM vs .64-NNI and .22-TLI for %REC). In addition, the WAM method allowed for the quantification of nCBV from 2 and 5 samples where the nonlinear fitting failed to calculate voxels on an individual basis using the NNI and TLI methods respectively.

Relationship to Vascular Morphology: Histograms illustrating the distribution of nCBV calculated from each of the 3 pre-processing strategies within tissue samples of simple (N=33, red) and complex (N=31, blue) vascular morphologies are displayed in Figure 1B. Since samples were targeted for the presence of tumor, there were not enough delicate samples (N=15) to include in the analysis. Although the difference between the modes of the histograms of the different vascular morphologies were similar between methods, the WAM method (top) showed a separable pattern between simple and complex samples with a more uniform, unimodal distribution, whereas the NNI (middle) and TLI (bottom) methods resulted in higher overlap between vascular morphologies and lacked the presence of a central quantifiable peak.

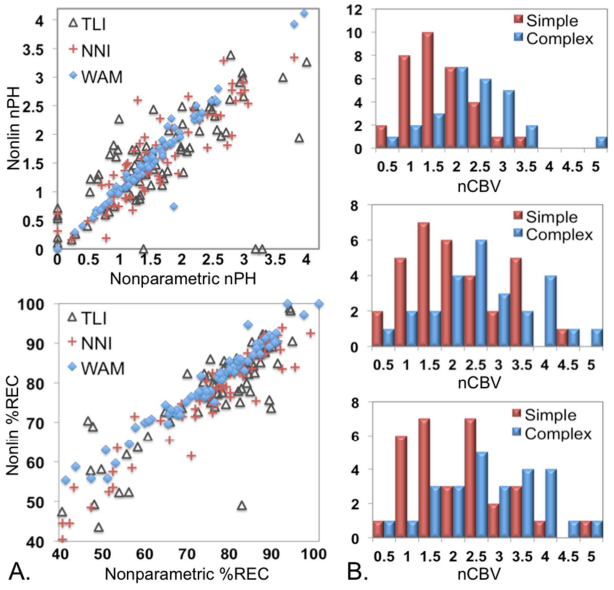

Figure 1. A. Scatter plots of nPH (top) and %REC (bottom) from nonlinear fitting vs nonparametric analysis for TLI, NNI, and WAM pre-processing methods. B. Histograms of nCBV values for tissue samples with simple (red) and complex (blue) vascular morphology for WAM (top), NNI (middle), and TLI (bottom) methods.

Conclusions

Our results indicate that the method for pre-processing DSC data highly influences the parameter values obtained from regions of image-guided tissue samples. Employing a pre-processing strategy that takes a weighted average of dynamic curves based on their percentage overlap with the tissue sample mask and excludes voxels with no signal was shown to be advantageous in minimizing variability in resulting metrics and more closely represented the underlying vascular morphology from histopathological tissue analysis compared to commonly used methods that resample the resolution.

Acknowledgements: NIH grants P50-CA97257 and P01CA118816

References: [1] Barajas RF et al. Neuro Oncol 2009, [2] Jain R et al. Acad Radiol 2011, [3] Essock-Burns E et al. JMRI 2012 [4] Paulson ES et al. Radiology 2008, [5] Hu LS et al. AJNR 2010 [6] Weisskoff RM. ISMRM 1994 [7] Rueckert D, et al. IEEE Trans Med Imaging 1999, [8] Lupo et al. AJNR 2005.